Synergetic Degradation of Rhodamine B at a Porous $ZnWO_4$ Film Electrode by Combined Electro-Oxidation and Photocatalysis

XU ZHAO AND YONGFA ZHU*

Department of Chemistry, Tsinghua University, Beijing, 100084, People's Republic of China

Synergetic degradation of rhodamine B (RhB) was investigated by combining electro-oxidation and photocatalysis using porous $ZnWO_4$ film at various bias potentials. The applied bias potential below 0.8 V enhanced the photocatalytic degradation of RhB by promoting the separation and transfer of photogenerated holes and electrons. At the potential between 0.8 and 1.0 V, the degradation of RhB was further enhanced, which is induced by direct electro-oxidation and photocatalysis. At the potential greater than 1.3 V, indirect electro-oxidation of RhB occurred with the largest synergetic effect. The synergetic effect can also increase the mineralization degree of the RhB. On the basis of the X-ray photoelectron spectra (XPS) analysis of the surface of the electrode after electrochemical reaction, the electropolymerization occurred which blocked the electrode and slowed the electro-oxidation of RhB. Active species generated via the photocatalytic process can activate the passivated electrode and promote the electro-oxidation of RhB. The O_2 electrochemically generated at the anode promoted the photocatalysis by capturing the photogenerated electrons and may induce the formation of H_2O_2. Thus, more active species could be formed through new reactive routines in the photoelectrocatalytic (PEC) process. RhB degradation was mainly through decomposition of the conjugated chromophore structure with slight occurrence of de-ethylation. The stability of the electrode in the PEC process was confirmed based on the XPS and Raman analysis.

Introduction

Photoelectrocatalytic (PEC) oxidation has been proven an efficient method in degrading organic contaminants in aqueous solutions (*1*−*5*). In this process, the low electrical bias potential applied between the anode and cathode is used to prevent charge recombination; the electrochemical degradation of the target contaminants is usually avoided.

Recently, electrochemical techniques have been extensively studied in degrading organic contaminants in aqueous solution due to their easy applicability to automation, high efficiency, and environmental compatibility (*6*−*9*). Although various types of electrodes with high O_2 evolution overpotential have been developed (*7*), the main problem hindering their large-scale application in wastewater treatment is the high electric energy consumption mainly caused by the side reaction of oxygen evolution. Moreover, electrode passivation is of susceptibility because of electropolymerization and fouling as summarized in the literature (*8*, *9*), which decreases the electro-oxidation efficiency.

It is known that the O_2, acting as a scavenger of photogenerated electrons, is beneficial for the photocatalytic degradation of organic contaminants. Moreover, the photocatalytic reaction occurring on the photoanode surface could induce the formation of active radicals, which may activate the electrode. Since the strengths of electro-oxidation and photocatalysis are complementary, a system that employs them both seems a worthwhile endeavor. Pelegrini et al. and Pinhedo et al. observed a synergetic effect for the photo-assisted electrochemical degradation of organic pollutants on a 70%TiO_2/30%RuO_2-coated titanium (Ti) anode (*10*, *11*); Quan et al. reported the synergetic effect in degrading 2,4-dichlorophenoxyacetic acid by integrated photo- and electrochemical catalysis on a Pt-doped TiO_2/Ti electrode (*12*); An et al. also indicated the synergetic effect in the degradation of formic acid using a PEC reactor with a porous Ti plate electrode (*13*). Although these studies reflect the potential of combining electro-oxidation and photocatalysis, the use of these composite electrode materials cannot employ the advantages of electro-oxidation and photocatalysis efficiently. Furthermore, the synergetic effect is not fully understood. Therefore, better understanding of the synergetic mechanism and development of new electrode materials are necessary.

Herein, using porous $ZnWO_4$ films as anode, a significant synergetic effect was observed in degrading rhodamine B (RhB) via combined electro-oxidation and photocatalysis. At different bias potentials the synergetic effect was induced via the different pathways, and the synergetic mechanism is discussed in detail. $ZnWO_4$ is an important inorganic material because of its luminescence behavior, structure properties, and potential applications such as photoluminescence, scintillator materials, and heterogeneous catalysis (*14*). However, application of the $ZnWO_4$ film in PEC degradation of organic contaminants has not been reported. The obtained results indicate that the porous $ZnWO_4$ film not only can photocatalytically degrade RhB under UV light irradiation but also can electrochemically degrade RhB efficiently. Moreover, the porous $ZnWO_4$ film is relatively stable. Because the degradation process of RhB (the molecular structure shown below) has been investigated in detail (*15*−*18*), it is convenient to use it to test PEC activity of the $ZnWO_4$ film electrode and investigate the synergetic effect.

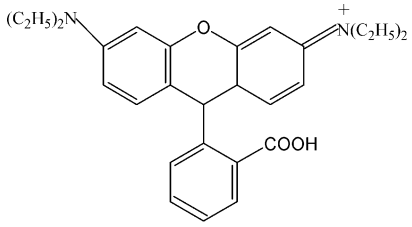

Rhodamine-B

Experimental Section

Preparation and Characterization of the Porous $ZnWO_4$ Film. Indium−tin oxide (ITO) glass (thickness, 1.1 mm; a sheet resistance, 15 Ω) was purchased from China Southern Glass Co. Ltd. All other chemicals are of analytical grade and used without further purification. Deionized water was used throughout the experiment. Porous $ZnWO_4$ films with a thickness of ca. 45 nm were prepared on the ITO glass from

* Corresponding author phone: +86-10-62783586; fax: +86-10-62787601; e-mail: zhuyf@mail.tsinghua.edu.cn.

10.1021/es052029e CCC: $33.50
Published on Web 04/11/200

an amorphous heteronuclear complex via a dip-coating method as described previously (*19*). XPS spectra were obtained using a PHI Quantera SXM (PHI-5300/ESCA, ULVAC-PHI, INC). An Al Kα X-ray beam was used with a power of 250 W. The base vacuum of the chamber was maintained at 3×10^{-9} torr during XPS analysis. Prior to the measurement, the electrode was washed with water to remove electrolyte.

Degradation Experiments. Degradation of RhB was performed in a PEC system as shown in the Supporting Information (Figure S1). The reactor (50 mm × 50 mm × 140 mm) was placed 3 cm away from a 15 W germicidal lamp (~90% of energy output at 253.7 nm). The intensity of light, as measured by a UV-irradiance meter (Instruments of Beijing Normal University), was 14 μW/cm^2 at the position where the film electrode was placed. Electro-oxidation and the PEC reaction employed a CHI660B electrochemical system (Shanghai, China) connected with a counter electrode (Pt wire, 70 mm in length with a 0.4 mm diameter), a working electrode (the $ZnWO_4$ film, active area of 14 cm^2), and a reference electrode (a saturated calomel electrode, SCE). The electrolyte solution of 0.5 mol/L Na_2SO_4 was used. Electrochemical impedance spectra (EIS) were recorded in the potentiostatic mode. The amplitude of the sinusoidal wave was 10 mV, and frequency range of the sinusoidal was from 100 kHz to 0.05 Hz.

RhB solution (100 mL) with an initial concentration of 5 mg/L was sampled periodically during the reaction to check the degree of decoloration, which was done by measuring the absorbance at 550 nm as a function of reaction time using a Shimazu S 2600 UV spectrophotometer. A total organic carbon (TOC) analyzer (TOC-V_{wp}, Shimadzu, Japan) was employed for determining the mineralization of RhB solutions. Prior to injection into the TOC analyzer, 50 mL was collected from the aqueous solutions and filtered with a 0.45 μm Millipore filter. All experiments were carried out at least twice. The reported values are within the experimental error of ±3%. The de-ethylation intermediates of RhB were determined by a high-performance liquid chromatography (HPLC) system, which consisted of a Dionex P580 pump, a UVD 340S diode array detector, and an Intersil ODS-3 C_{18} reverse column (5 μm, 250 × 4.6 mm^2).

Results and Discussion

Photocatalytic Degradation of RhB. As shown in Figure 1A, the degradation rate of RhB increased in the presence of the $ZnWO_4$ film in comparison with the direct photolysis of RhB. An amount of 71% of RhB was removed using the $ZnWO_4$ film against 62% removed by the TiO_2 film (55 nm thickness) within 4 h, which was prepared via a sol−gel process by the dip-coating method (*20*). It is well established that the photocatalytic degradation of organic contaminants fits the pseudo-first kinetic equation when the concentration of the contaminants is low, and the pseudo-first kinetic constants of RhB degradation under various conditions (Table S1, Supporting Information) support the high photocatalytic activity of the porous $ZnWO_4$ film.

The wider band gap of the $ZnWO_4$ film than that of the TiO_2 film (Figure S2, Supporting Information) contributed to a more powerful redox capability. Its porous structure (Figure S3, Supporting Information) offers more active sites to adsorb water and hydroxyl groups, which capture holes generated by illumination and produce active hydroxyl radicals. The porous structures also offer an advantage in that the diffusion length of the valence band holes formed by the band gap photoexcitation is short, because the electrolyte solution can penetrate into the pores in the whole film (*21*). All of these factors contribute to the high photocatalytic activity of the porous $ZnWO_4$ film.

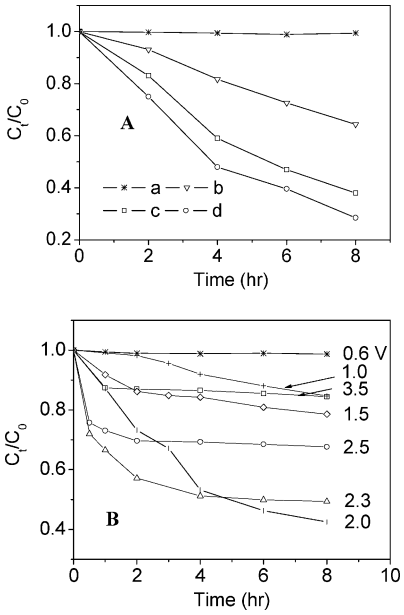

FIGURE 1. (A) Relative concentration variation of RhB with irradiation time: dark control (a); direct photolysis (b); photocatalytic degradation using TiO_2 film (55 nm) (c) and $ZnWO_4$ film (45 nm) (d). C_t/C_0 = concentration at time *t*/initial concentration. (B) Concentration variation of RhB in electrochemical degradation at various potentials in 0.5 M Na_2SO_4 solution.

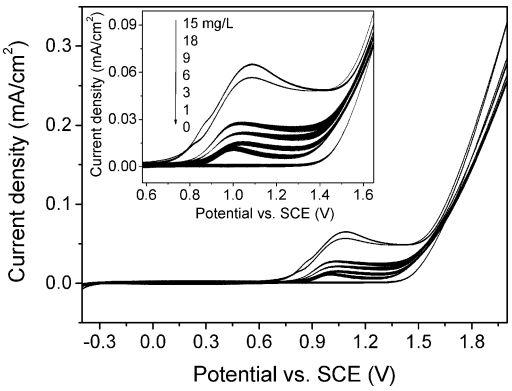

FIGURE 2. Cyclic voltammetry scans with the $ZnWO_4$ film electrode in a 0.5 M Na_2SO_4 electrolyte with various concentrations of RhB at a pH value of 6.

Electrochemical Degradation. Figure 1B shows the concentration variation of RhB at various bias potentials of 0.5, 1.0, 1.5, 2.0, 2.3, 2.5, and 3.5 V, respectively. At the potential of 1.0 V, the degradation of RhB is observable, and the degradation rate increases as a function of the bias potential up to 2.0 V. It is found that RhB degradation fits the pseudo-first kinetic equation at the bias potentials of 1.0, 1.5, and 2.0 V. Correspondingly, the rate constants are 0.022, 0.026, and 0.138 hr^{-1} respectively (Table S1). Furthermore, the degradation rate of RhB slows down with the increase of applied bias. Moreover, nearly no degradation of RhB is observed at 3.5 V after the initial 1 h.

The cyclic voltammetry scans of the $ZnWO_4$ film in the 0.5 M Na_2SO_4 solution without RhB and with various concentrations of RhB are presented in Figure 2. At the potential of ca. 1.0 V, the current densities increase with the concentration of RhB up to 15 mg/L. But it decreases when the concentration of RhB was 18 mg/L, which is due to the heavier block at higher RhB concentration. The current is generated from the direct electro-oxidation of RhB. When the potential exceeds 1.4 V, the anodic currents increased largely with the potential, which may result from electro-

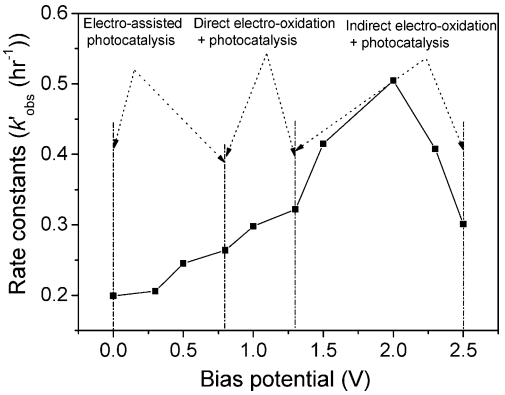

FIGURE 3. Degradation rate constants of RhB vs applied bias potential under UV light irradiation (light intensity of 14 μW/cm^2, RhB concentration of 5 mg/L).

oxidation of RhB plus the evolution of oxygen. With the evolution of oxygen, the active species such as hydroxyl radicals (·OH), H_2O_2, or O_3 can be formed (*22*), which lead to the indirect oxidation of RhB. Most of researchers agree with the "hydroxyl radical oxidation" mechanism for the indirect electrochemical degradation of organic contaminants (*23*−*25*).

$$MOx + H_2O \rightarrow MOx\ [\cdot OH] + H^+ + e^- \quad (1)$$

$$MOx\ (\cdot OH) + D \rightarrow XCO_2 + xe^- + zH^+ \quad (2)$$

$$MOx\ (\cdot OH) + D \rightarrow {}^1/_2O_2 + e^- + MO_X \quad (3)$$

where D stands for the target contaminants.

Further, it can be seen from Figure 1B that the electrochemical degradation of RhB was fast within the initial 2 h. With the extension of reaction time, the degradation rate decreased. Moreover, at a potential greater than 2.0 V, only slight degradation or no degradation of RhB was observed after the initial 2 h. A similar phenomenon in electrochemical degradation of wethylparathion was observed by Vlyssides et al. (*6*) and Pelegrino et al. (*26*). Vlyssides et al. considered that after the original oxidation of wethylparathion some materials, which were deposited on the electrode, blocked further access of the wethylparathion to the electrode surface, slowing down the wethylparathion degradation. However, Pelegrino et al. argued that the slow degradation was due to the mechanism of contaminants oxidation with simultaneous oxygen evolution (*11*). As for our case, the explanation will be given in detail subsequently.

Combined Electro-Oxidation and Photocatalysis. PEC degradation of RhB was performed at potentials of 0, 0.3, 0.5, 0.8, 1.0, 1.3, 1.5, 2.0, 2.3, 2.5, and 3.5 V, respectively. The variation of relative concentration (C_t/C_0) of RhB as a function of time is selectively shown in Figure S4, in the Supporting Information. It is well established that PEC degradation of organic contaminants fit the pseudo-first kinetic equation when the concentration of the contaminants is low. The pseudo-first kinetic constants versus various applied bias potentials are given in Figure 3.

It is clearly shown that the bias potential at 0, 0.3, and 0.5 V can promote the photocatalytic degradation effectively. The degradation rate of RhB was further increased at the bias potential of 1.0 V and reached the largest value at the bias potential of 2.0 V. However, the degradation rate of RhB decreased at 2.3 V; it was further decreased at 2.5 V. Furthermore, it is observed that the kinetic constants of the PEC process at 1.0 and 2.0 V are beyond the sum of the electrochemical degradation or photocatalytic process individually. A similar conclusion can be drawn by considering

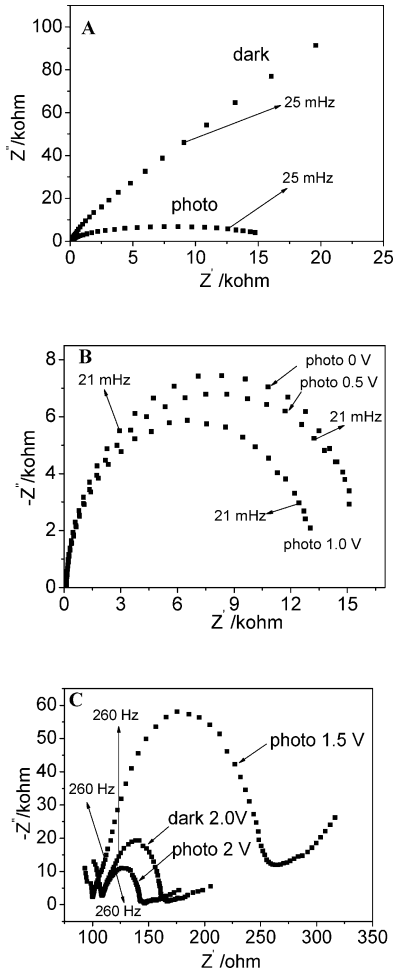

FIGURE 4. Effect of photoirradiation and the applied bias potential on the EIS plane display of the degradation of RhB at the $ZnWO_4$ film electrode; the amplitude of the sinusoidal wave was 10 mV, and the frequency range of the sinusoidal was 100 kHz to 0.05 Hz.

the reduction of TOC content. At the potential of 2.0 V, after a reaction of 4 h, the individual electrochemical and photocatalytic processes permitted TOC reduction of 28% and 35%, respectively, while the PEC process led to a TOC reduction of 81%. Thus, the synergetic effect not only increased the degradation rate but also enhanced the mineralization of RhB.

Synergetic Mechanism. Figure 4A shows the EIS response of the $ZnWO_4$ film electrode under dark and photoirradiation conditions. It is clear that the size of the arc radius on the EIS Nynquist plot is largely reduced due to the photoirradiation. Furthermore, the sizes of the arc radius are reduced by applying the applied potentials of 0.5 and 1.0 V (Figure 4B). The size of the arc radius on the EIS Nynquist plot reflects the rate of the electrode reaction (*27*, *28*). These results confirmed that the applied bias increased the degradation rate of RhB. In addition, only one arc can be observed on the Nynquist plot, which suggested that the electro-oxidation, photocatalysis, and PEC reaction appear to be a simple electrode process (*27*).

However, as shown in Figure 4C, the sizes of the arc radius are largely reduced under application of 2.0 V bias potential or combination of photoirradiation and applied bias potential of 1.5 and 2.0 V. It is the smallest at the 2.0 V applied potential combined with photoirradiation, which means an effective separation of the photogenerated electron−hole pair and a fast interfacial charge transfer to the electron donor/electron acceptor as suggested by Leng et al. (*28*). Thus, RhB can be

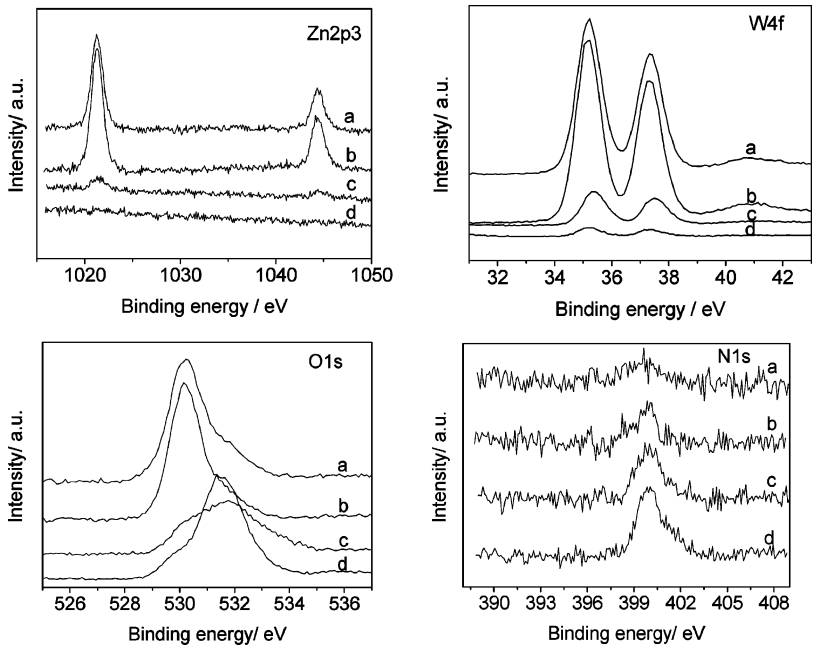

FIGURE 5. XPS of $ZnWO_4$ film (a) before and (b) after PEC reaction (2.0 V), (c) electro-oxidation (2.0 V), and (d) electro-oxidation (3.5 V) in 0.5 M $NaSO_4$ solution with 5 mg/L RhB (24 h reaction, light intensity of 14 μW/cm^2).

effectively degraded. Moreover, the Nynquist plot shapes are largely changed, indicating that different reactive mechanisms are involved.

The redox potential of RhB is determined to be ca. 1.0 V as shown in Figure 2 in our case. Below this potential, the potential of 0, 0.3, and 0.5 V increases the photocatalytic degradation rate of RhB by promoting the separation and transfer of photogenerated holes and electrons. At the bias potential of 1.0 V, the direct electro-oxidation of RhB occurs as discussed above. The applied bias potential not only can separate the holes and electrons but also can directly electrolyze RhB. The integrated degradation of RhB was through the direct electro-oxidation and photocatalysis.

At a potential greater than 1.4 V, the water discharges on the electrode surface (as show in Figure 2) may lead to the formation of ·OH (*29*, *30*) by eqs 1 and 2 and O_2 by eq 3. In these cases, the indirect electro-oxidation of RhB occurs. Moreover, O_2 as an acceptor of electrons by eq 4 may promote the photocatalysis of RhB. The increase of the dissolved oxygen in the solution induced by the electrochemical evolution of oxygen at the anode may promote the production of H_2O_2 at the cathode surface by eq 4. The H_2O_2 tends to have a lower activity than ·OH radicals and does not degrade RhB efficiently as confirmed by Masui et al. (*31*). However, the ·OH radicals can be formed through UV light excitation of the H_2O_2 (*32*) by eq 5. H_2O_2 can also react with photogenerated electrons and generate ·OH by eq 6. Thus, the degradation of RhB can be carried out via many reactive routines, including their combination.

$$O_2 + 2H^+ + 2e^- \rightarrow H_2O_2 \quad (4)$$

$$H_2O_2 + h\nu \rightarrow 2{\cdot}OH \quad (5)$$

$$H_2O_2 + e^- \rightarrow {\cdot}OH + OH^- \quad (6)$$

The XPS analysis as shown in Figure 5 indicated that the change in intensity of Zn, W, and O for the film sample used in the PEC process (2.0 V) within 24 h is unnoticeable. However, the intensity greatly decreases for the film sample used in the electrochemical process at the same condition. Moreover, the binding energy of the O changed, and a certain amount of nitrogen was observed. This behavior can be attributed to the passivation of the electrode by an anodically deposited film. It is well-known that inactivation of the electrode is susceptible due to electropolymerization reactions and fouling (*8*, *9*). For example, it is confirmed that electro-oxidation of phenol or chlorinated phenols can form polymeric products, which have low solubility in aqueous media and are adsorbed on electrode surfaces, passivating them from further reaction (*8*). Various approaches have been used to weaken the electrode fouling including removing them from the electrode surface, chemically modifying the electrode surface, and optimizing the electro-oxidation conditions. In our case, with the UV radiation incident on the electrode surface for the PEC process, the $ZnWO_4$ is excited and ·OH intermediate species are formed, which not only lead to the photocatalytic degradation of RhB but also activate the electrode surface and promote the electrochemical and PEC degradation of RhB. Figure S5A in the Supporting Information shows the progressive scanning between −1.0 and 1.5 V for three cycles. The first cycle shows a well-defined peak corresponding to the direct electrochemical degradation of RhB at approximate 1.0 V, which decreases drastically in subsequent cycles. However, after UV irradiation for 20 min, the current density at the same potential increased as shown in the Figure S5B. These results further supported the above conclusions.

When the bias potential exceeds 2.0 V, the synergetic effect decreases gradually (Table S1). This phenomenon is consistent with that of electrochemical degradation of RhB (Figure 1B). Pinhedo et al. observed the same phenomena in PEC degradation of humic acid on a $(TiO_2)_{0.7}(RuO_2)_{0.3}$ dimensionally stable anode (*11*). They consider that the overpotential for oxygen evolution reaction increases with the current density. Thus, most of the ·OH radicals formed further react to form oxygen by eq 3. To further explore the reason, the electrode surface was analyzed by XPS. As shown in Figure 5, the peak intensities of W and Zn decrease and the amounts of nitrogen increase, and the binding energy of O changes largely for the electro-oxidation at 3.5 V in contrast to that at 2.0 V. The deposited film can be formed on the electrode surface during the electrochemical and PEC degradation of RhB as suggested above. The faster orininal

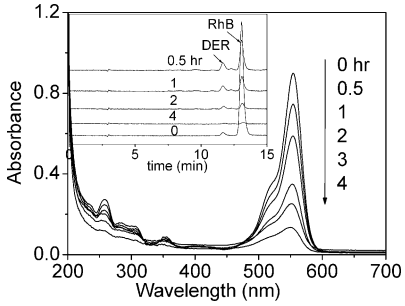

FIGURE 6. UV−vis spectrum and HPLC chromatograms (inset) of RhB solution at various time intervals for the PEC degradation process with an applied bias potential of 2.0 V.

oxidation of RhB at higher potential leads to the formation of more intermediates, which were deposited on the electrode surface, blocking further access of RhB and slowing the RhB degradation. Additionally, the electrode was analyzed by Raman spectroscopy. As shown in Figure S6 in the Supporting Information, nearly no change was observed on the film electrode after electro-oxidation for 24 h at 2.0 or 3.5 V, which excludes the possible destruction of the $ZnWO_4$ film electrode.

Degradation Mechanism of RhB and Stability of the Film Electrode. The degradation process of RhB has been investigated in detail previously (*15*, *16*). It is recognized that diminishment of the absorption band of RhB at 551 nm indicates decomposition of the conjugated xanthene ring in RhB; hypsochromic shift of the band is due to the stepwise de-ethylation of the *N*,*N*′-diethylammonium groups in the RhB structure. In our case, no obvious shift of absorbance at 551 nm is observed during the combined electro-oxidation and photocatalysis as selectively shown in Figure 6. RhB used in our case is of 95% purity with an *N*,*N*-diethyl-*N*′-ethyl-rhodamine (DER) percentage of ca. 5%. In the inset of Figure 6, with the quick disappearance of RhB, the concentration of DER increased slightly and then decreased with further PEC reaction. This proved that de-ethylation of RhB occurred, but it was not the dominant process. Decomposition of the conjugated chromophore structure of RhB should be the major process. The degradation process of RhB is similar with that of its PEC oxidation at a Ti/TiO_2 mesh electrode (*17*). The UV−vis spectrum changes of RhB during the photocatalysis and electro-oxidation are similar with those of the PEC process. Therefore, it could be concluded that the degradation of RhB in these processes was also mainly through the decomposition of the conjugated xanthene.

There is no noticeable change in the XPS and Raman spectrum of the $ZnWO_4$ film after 24 h of PEC reaction at 2.0 V bias potential (Figure S6). Furthermore, PEC degradation of RhB was performed for five times at the bias potential of 2.0 V for 4 h; the results indicated that the degradation efficiencies were rather stable with the relative standard deviation of 3.1% (Figure S6). It is considered that the observed chemical stability of the $ZnWO_4$ film electrode led to the stable catalytic activities. Although the $ZnWO_4$ film with a band gap of 4.06 eV is not suitable in regard to solar light emission, its wide band gap can contribute to strong redox ability, which is beneficial for the oxidation and reduction of the target contaminant. Moreover, $ZnWO_4$ with complex structure is suitable for doping another cation/anion to induce its visible light response.

Acknowledgments

This work was partly supported by National Natural Science Foundation of China (20433010, 20507011), the Trans-Century Training Program Foundation for the Talents by the Ministry of Education, P.R.C, the Excellent Young Teacher Program of MOE, P. R. China, and the Chinese Postdoctoral Foundation (023204337). We acknowledge the help from Hongwei Ji on HPLC analysis of RhB degradation intermediates and from Jincai Zhao on discussion of its degradation mechanism.

Supporting Information Available

PEC reactive system (Figure S1), structure and texture of the $ZnWO_4$ film (Figures S2 and S3), variation of relative concentration of RhB under various conditions (Figure S4), cyclic voltammetry scans with the film electrode in a 0.5 M Na_2SO_4 electrolyte with 5 mg/L RhB before and after photoirradiation (Figure S5), Raman spectra variation of the $ZnWO_4$ film during variously reactive processes (Figure S6), and pseudo-first-order rates of RhB degradation under various conditions (Table S1). This material is available free of charge via the Internet at http://pubs.acs.org.

Literature Cited

(1) Vinodgopal, K.; Hotchandani, S.; Kamat, P. V. Electrochemically assisted photocatalysis. TiO_2 particulate film electrodes for photocatalytic degradation of 4-chlorophenol. *J. Phys. Chem.* **1993**, *97*, 9040−9044.

(2) Kim, D. H.; Anderson, M. A. Photoelectrocatalytic degradation of formic acid using a porous titanium dioxide thin-film electrode. *Environ. Sci. Technol.* **1994**, *28*, 479−483.

(3) Candal, R. J.; Zeltner, W. A.; Anderson, M. A. Effects of pH and applied potential on photocurrent and oxidation rate of saline solutions of formic acid in a photoelectrocatalytic reactor. *Environ. Sci. Technol.* **2000**, *34*, 3443−3451.

(4) Li, X. Z.; Liu, H. S. Development of an E-H_2O_2/TiO_2 photoelectrocatalytic oxidation system for water and wastewater treatment. *Environ. Sci. Technol.* **2005**, *39*, 4614−4620.

(5) Quan, X.; Yang, S. G.; Ruan, X. L.; Zhao, H. M. Preparation of titania nanotubes and their environmental applications as electrode. *Environ. Sci. Technol.* **2005**, *39*, 3770−3775.

(6) Vlyssides, A.; Barampouti, E. M.; Mai, S.; Arapoglou, D.; Kotronarou, A. Degradation of methylparathion in aqueous solution by electrochemical oxidation. *Environ. Sci. Technol.* **2004**, *38*, 6125−6131.

(7) Chen, G. H. Electrochemical technologies in wastewater treatment. *Sep. Purif. Technol.* **2004**, *38*, 11−41.

(8) Muna, G. W.; Tasheva, N.; Swain, G. M. Electro-oxidation and amperometric detection of chlorinated phenols at boron-doped diamond electrodes: a comparison of microcrystalline and nanocrystalline thin films. *Environ. Sci. Technol.* **2004**, *38*, 3674−3682.

(9) Marselli, B.; Garcia-Gomez, J.; Michaud, P.-A.; Rodrigo, M. A.; Comninellis, C. Electrogeneration of hydroxyl radicals on boron-doped diamond electrodes. *J. Electrochem. Soc.* **2003**, *150*, 79−83.

(10) Pelegrini, R. T.; Freire, R. S.; Duran, N.; Bertazzoli, R. Photo-assisted electrochemical degradation of organic pollutants on a DSA type oxide electrode: process test for a phenol synthetic solution and its application for E1 bleach kraft mill effluent. *Environ. Sci. Technol.* **2001**, *35*, 2842853.

(11) Pinhedo, L.; Pelegrini, R.; Bertazzoli, R.; Motheo, A. J. Photo-electrochemical degradation of humic acid on a $(TiO_2)_{0.7}(RuO_2)_{0.3}$ dimensionally stable anode. *Appl. Catal., B* **2005**, *57*, 75−81.

(12) Quan, X.; Chen, S.; Su, J.; Chen, J. W.; Chen, G. H. Synergetic degradation of 2,4-D by integrated photo- and electrochemical catalysis on a Pt doped TiO_2/Ti electrode. *Sep. Purif. Technol.* **2004**, *34*, 73−79.

(13) An, T. C.; Xiong, Y.; Li, G. Y.; Zhao, C. H.; Zhu, X. H. Synergetic effect in degradation of formic acid using a new photoelectrochemical reactor. *J. Photochem. Photobiol., A* **2002**, *152*, 155−165.

(14) Yu, S. H.; Liu, B.; Mo, M. S.; Huang, J. H.; Liu, X. M.; Qian, Y. T. General synthesis of single-crystal tungstate nanorods/nanowires: a facile, low-temperature solution approach. *Adv. Funct. Mater.* **2003**, *13*, 639−647.

(15) Lei, P. X.; Chen, C. C.; Yang, J.; Ma, W. H.; Zhao, J. C.; Zang, L. Degradation of dye pollutants by immobilized polyoxometalate with H_2O_2 under visible-light irradiation. *Environ. Sci. Technol.* **2005**, *39*, 8466−8474.

(16) Chen, C. C.; Zhao, W.; Lei, P. X.; Zhao, J. C.; Serpone, N. Photosensitized degradation of dyes in polyoxometalate solutions versus TiO_2 dispersions under visible-light irradiation: mechanistic implications. *Chem. Eur. J.* **2004**, *10*, 1956−1965.

(17) Li, X. Z.; Liu, H. L.; Li, F. B.; Mak, C. L. Photoelectrocatalytic oxidation of rhodamine B in aqueous solution using Ti/TiO_2 mesh photoelectrodes. *J. Environ. Sci. Health, Part A* **2002**, *37*, 55−59.
(18) Park, H.; Choi, W. Photocatalytic reactivities of Nafion-coated TiO_2 for the degradation of charged organic compounds under UV or visible light. *J. Phys. Chem. B* **2005**, *109*, 11667−11674.
(19) Zhao, X.; Wu, Y.; Zhang, S. C.; Zhu, Y. F. Fabrication and photoelectrochemical properties of porous $ZnWO_4$ film. *J. Solid State Chem.*, in revision.
(20) Shang, J.; Li, W.; Zhu, Y. F. Structure and photocatalytic characteristics of TiO_2 film photocatalyst coated on stainless steel webnet. *J. Mol. Catal. A: Chem.* **2003**, *202*, 187−195.
(21) Wang, X. C.; Yu, J. C.; Hou, Y. D.; Fu, X. Z. Three-dimensionally ordered mesoporous molecular-sieve films as solid superacid photocatalysts. *Adv. Mater.* **2005**, *17*, 99−101.
(22) Michaud, P. A.; Panizza, M.; Quattara, L.; Diaco, T.; Foti, G.; Comninellis, C. Electrochemical oxidation of water on synthetic boron-doped diamond thin film anodes. *J. Appl. Electrochem.* **2003**, *33*, 151.
(23) Zhou, M.; Dai, Q.; Lei, L. C.; Ma, C.; Wang, D. Long life modified lead dioxide anode for organic wastewater treatment: electrochemical characteristics and degradation mechanism. *Environ. Sci. Technol.* **2005**, *39*, 363−370.
(24) Kesselman, J. M.; Weres, O.; Lewis, N. S.; Hoffmann, M. R. Electrochemical production of hydroxyl radical at polycrystalline Nb-doped TiO_2 electrodes and estimation of the partitioning between hydroxyl radical and direct hole oxidation pathways. *J. Phys. Chem. B* **1997**, *101*, 2637−2643.
(25) Comninellis, C.; De Battisti, A. Electrocatalysis in anodic oxidatives of organic with simultaneous oxygen evolution. *J. Chim. Phys. Phys.-Chim. Biol.* **1996**, *93*, 673−679.
(26) Pelegrino, R. R. L.; Vicentin, L. C.; De Andrade, A. R.; Bertazzoli, R. Thirty minutes laser calcination method for the preparation of DSA (R) type oxide electrodes. *Electrochem. Commun.* **2002**, *4*, 139−142.
(27) Liu, H.; Cheng, S.; Wu, M.; Wu, H.; Zhang, J.; Li, W.; Cao, C. Photoelectrocatalytic degradation of sulfosalicylic acid and its electrochemical impedance spectroscopy investigation. *J. Phys. Chem. A* **2000**, *104*, 7016−7020.
(28) Leng, W. H.; Zhang, Z.; Zhang, J. Q.; Cao, C. N. Investigation of the kinetics of a TiO_2 photoelectrocatalytic reaction involving charge transfer and recombination through surface states by electrochemical impedance spectroscopy. *J. Phys. Chem. B* **2005**, *109*, 15008−15023.
(29) Simond, O.; Schaller, V.; Comninellis, C. Theoretical model for the anodic oxidation of organics on metal oxide electrodes. *Electrochim. Acta* **1997**, *42*, 2009−2012.
(30) Pelegrini, R.; Reyes, J.; Duran, N.; Zamora, P. P.; De Andrade, A. R. Photoelectrochemical degradation of lignin. *J. Appl. Electrochem.* **2000**, *30*, 953−958.
(31) Masui, T.; Watanabe, F.; Yamagishi, A. Temperature-jump study on the aquation of iron (III) complex by dodecylpyridinium chloride-solubilized water in chloroform. *J. Phys. Chem.* **1977**, *81*, 494−496.
(32) Chen, J. S.; Liu, M. C.; Zhang, L.; Zhang, J. D.; Jin, L. T. Application of nano TiO_2 towards polluted water treatment combined with electro-photochemical method. *Water Res.* **2003**, *37*, 3815−3820.

Received for review October 14, 2005. Revised manuscript received March 3, 2006. Accepted March 15, 2006.

ES052029E